

## Exceptional-Point Phase Transition in Coupled Magnonic Waveguides

Alexander V. Sadovnikov,<sup>1,2</sup> Alexander A. Zyablovsky<sup>1,2,3,4,5,\*</sup>, Alexander V. Dorofeenko<sup>1,2,3,4,5</sup> and Sergey A. Nikitov<sup>1,2,4,†</sup>


<sup>1</sup>Laboratory “Metamaterials”, Saratov State University, 83 Astrakhanskaya, Saratov 410012, Russia

<sup>2</sup>Kotelnikov Institute of Radioengineering RAS, 11-7 Mokhovaya, Moscow 125009, Russia

<sup>3</sup>Dukhov Research Institute of Automatics (VNIIA), 22 Sushchevskaya, Moscow 127055, Russia

<sup>4</sup>Moscow Institute of Physics and Technology, 9 Institutskiy pereulok, Moscow 141700, Russia

<sup>5</sup>Institute for Theoretical and Applied Electromagnetics, 13 Izhorskaya, Moscow 125412, Russia

 (Received 2 March 2022; revised 16 July 2022; accepted 9 August 2022; published 26 August 2022)

Spontaneous symmetry breaking is a source of the phase transition in a variety of physical systems including such as non-Hermitian. It has recently been demonstrated that so-called exceptional points, which are singularities in non-Hermitian systems, separate the areas with symmetrical and asymmetrical eigenstates. Such separation is evidence of phase transitions in non-Hermitian systems taking place at exceptional points. In this paper, we experimentally demonstrate that exceptional-point phase transition in a system of two coupled magnonic waveguides coupled by dipole-dipole interaction occurs. Using infrared laser irradiation to control the spin-wave losses in one of the waveguides covered by a semiconductor GaAs layer, we observe a change in the wave numbers of the propagating spin waves and a change in the distribution of spin-wave intensity between the waveguides. Retrieving the experimental data, we find the spin-wave propagation parameters and, based on these and the use of coupled mode theory, we argue that in the system of magnonic waveguides the exceptional-point phase transition is observed.

DOI: [10.1103/PhysRevApplied.18.024073](https://doi.org/10.1103/PhysRevApplied.18.024073)

### I. INTRODUCTION

Non-Hermitian systems with exceptional points (EPs) are of great interest [1–6], which is due both to the desire to extend quantum mechanics to non-Hermitian systems [1–4] and to phenomena that take place in such systems [5,6]. Among non-Hermitian systems,  $PT$ -symmetric systems have been most studied. For such systems, a breaking of the  $PT$  symmetry of eigenstates has recently been predicted [1–4]. In recent years,  $PT$ -symmetry breaking has been investigated in optics [5–19], acoustics [5,20], and magnetism [21–24].  $PT$ -symmetry breaking occurs at a so-called exceptional point in the system parameter space. At the EP, two eigenstates become identical, which is possible due to the system’s non-Hermiticity. This corresponds to a maximal degree of nonorthogonality of these eigenstates [5,6,19]. Further, the phase transitions associated with the EPs have been demonstrated in various classical and quantum non-Hermitian systems without  $PT$ -symmetry [5,6,19,25], in particular, systems maintained far from thermal equilibrium [26]. The non-Hermitian systems possess a set of unusual properties near the EPs [5,6,19,25], which paves the way to creating alternative

types of lasers [27–33], sensors [34–37], and waveguides [14,38–40].

In magnetic systems, phase transition associated with the EP has been observed in a three-layer structure comprising thin Co and NiFe layers separated by a Pt spacer and possessing different levels of loss [21]. Inter-layer coupling was varied by thickness of Pt spacer, making phase transition possible near the EP. A system incorporating loss and gain for propagating spin waves was theoretically proposed in Ref. [22], where a system of two ferromagnetic  $Y_3Fe_5O_{12}$  (YIG) waveguides separated by a Pt spacer was excited by a spin-transfer torque [41]. As a result, the spin-wave losses were increased in one waveguide and decreased in the other. In such a way, the possibility of reaching the EP was shown. In both cases, interlayer exchange Ruderman–Kittel–Kasuya–Yosida (RKKY) interaction [42] was considered as a mechanism of the magnetic layer coupling. This is one possible realization for observation of  $PT$ -symmetry and the EP in magnonics.

We propose another magnonic system for observation of the EP phase transition. It consists of two magnonic waveguides coupled by dipole-dipole interaction. We report on the observation of the EP phase transition in such a magnonic waveguide system. In contrast to previously reported observations of the EP in the absorption spectra

\*zyablovskiy@mail.ru

†nikitov@cplire.ru

associated with ferromagnetic resonance in magnetic layers [21], we propose a planar structure consisting of two ferromagnetic (YIG) waveguides separated by an air gap. Spin waves were excited by the microwave microstrip antenna in one of the waveguides. Generally, an observation of the EP phase transition requires control of the losses in at least one of the waveguides [21,22] or of the waveguides' coupling strength [43,44]. For this purpose, we covered both waveguides with a gallium arsenide (GaAs) semiconductor layer and illuminated it by infrared (IR) laser radiation [45], so that only one waveguide was exposed. With the use of Brillouin light scattering (BLS) spectroscopy, we have measured spatial distributions of the magnetization oscillations intensity in the waveguides. At a variation of the IR laser power, changes characteristic of EP phase transition were observed in the BLS data. By fitting these data, we have retrieved the dependences of complex wave numbers and waveguide eigenmodes in the coupled waveguides on the IR laser power. Based on these dependences we show that the EP phase transition takes place in such a magnonic system.

## II. THEORETICAL MODEL

Spin-wave dynamics in two coupled waveguides [shown in Fig. 1(a)] is described by the Landau-Lifshitz-Gilbert (LLG) equation of motion of magnetization [46],

$$\frac{\partial \mathbf{M}_{1,2}}{\partial t} = -\gamma \left[ \mathbf{M}_{1,2} \times \frac{\delta W}{\delta \mathbf{M}_{1,2}} \right] + \frac{\alpha}{M_0} \left[ \mathbf{M}_{1,2} \times \frac{\partial \mathbf{M}_{1,2}}{\partial t} \right], \quad (1)$$

where  $\mathbf{M}_{1,2}$  are the magnetization vectors in the waveguides  $S_1, S_2$ ;  $\gamma$  is the gyromagnetic ratio (2.8 MHz/Oe);  $W$  is the ferromagnetic free energy of the system of two coupled waveguides; and  $\alpha$  is the Gilbert phenomenological dissipation parameter, which is estimated as a ratio of the ferromagnetic resonance (FMR) linewidth to the FMR frequency,  $\alpha = \Delta f_{\text{FMR}}/f_{\text{FMR}}$ . In our measurements, we have obtained  $\Delta H = 0.54$  Oe at  $f_{\text{FMR}} = 9.7$  GHz, that is,  $\Delta f_{\text{FMR}} = 1.512$  MHz. As a result, we have  $\alpha = 1.6 \times 10^{-4}$ .

If the magnonic system includes both gain and loss [21,22], Eq. (1) may be invariant at parity operations, namely, at  $\mathbf{M}_1 \rightarrow -\mathbf{M}_2$ ,  $\mathbf{H}_1 \rightarrow \mathbf{H}_2$  ( $\delta W/\delta \mathbf{M}_{1,2}$ ) and time reversal ( $t \rightarrow -t$ :  $\mathbf{M}_{1,2} \rightarrow -\mathbf{M}_{1,2}$ ,  $\mathbf{H}_{1,2} \rightarrow -\mathbf{H}_{1,2}$ ). In this case, the system described by Eq. (1) is  $PT$ -symmetric, and the EP transition related to the  $PT$ -symmetry breaking can take place in it. However, an EP may be observed in more general class of magnonic systems, so that  $PT$  symmetry is not necessary. We demonstrate the EP in a system of two coupled lossy waveguides, which do not possess  $PT$  symmetry.

Along with the LLG equation, the Maxwell's equations and electromagnetic boundary conditions are used to find spin-wave dispersion and coupling between waves in the waveguides. Combining all equations, one can reach a set of Schrödinger-type equations for the wave amplitudes (see, for example, Ref. [47]):

$$i \frac{\partial A_{1,2}}{\partial t} + iv_{g,1,2} \left( 1 - i\alpha \frac{\omega}{\omega_0} \right) \frac{\partial A_{1,2}}{\partial x} + \frac{1}{2} \beta_{1,2} \frac{\partial^2 A_{1,2}}{\partial x^2} + \kappa A_{2,1} = 0, \quad (2)$$

where  $A_1$  and  $A_2$  are the spin-wave amplitudes,  $v_{g,1,2} = 2d(\omega_0^2/4\omega)\exp(-2k_{1,2}d)f(z)$  are the wave group velocities,  $\beta_{1,2} = (v_{g,1,2}/\omega)[v_{g,1,2} + \omega d]f(z)$  are the wave dispersion coefficients,  $\omega_0 = 4\pi\gamma M_0$ ,  $M_0$  is the saturation magnetization,  $d$  is the ferromagnetic film thickness,  $k_{1,2}$  are the real parts of the wave numbers in the first and second waveguides,  $f(z)$  is the function describing the spatial mode distribution in the waveguides due to their finite width (typically having sinusoidal character), and  $\kappa$  is a phenomenological dipole-dipole coupling parameter.

The analysis of Eqs. (2) can be carried out for the continuous-wave (CW) case in the coupled mode approximation [22,48]. In this approximation, the spin-wave amplitudes in the waveguides are represented as  $A_{1,2} = a_{1,2}(x) \cdot F_{1,2}(y, z)$ . Here,  $F_{1,2}(y, z)$  describes the spin-wave distribution in the section of the  $n$ th waveguide, and  $a_n(x)$  is the partial amplitude of the spin wave in the  $n$ th waveguide. Assuming that  $F_{1,2}(y, z)$  does not change along the waveguides, one may find that the spin-wave amplitudes

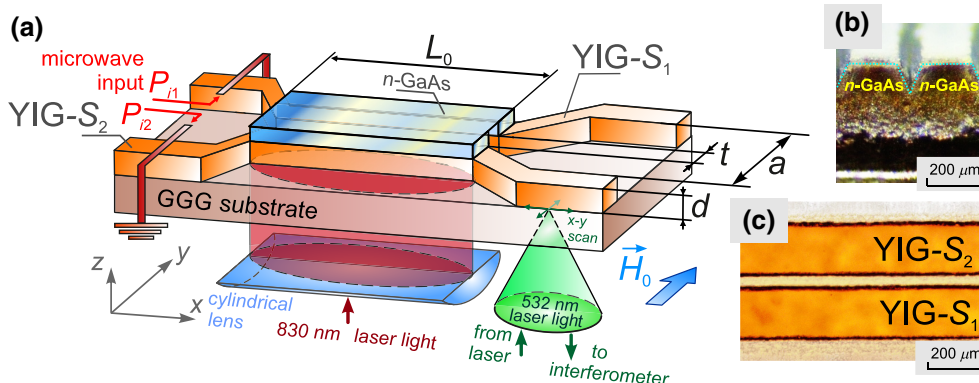


FIG. 1. (a) Schematic of the structure and of the experimental setup; (b) microphotograph of the GaAs profile; (c) microphotograph of adjacent YIG stripes ( $S_1$  and  $S_2$ ).

obey the following equations [22,48]:

$$\frac{d}{dx} \begin{pmatrix} a_1 \\ a_2 \end{pmatrix} = \hat{M} \begin{pmatrix} a_1 \\ a_2 \end{pmatrix}. \quad (3)$$

Here, the matrix  $\hat{M} = \begin{pmatrix} iq_1 & i\kappa \\ i\kappa & iq_2 \end{pmatrix}$  describes the propagation and interaction of the waveguide modes, and  $q_1 = k_1 + ig_1$  and  $q_2 = k_2 + ig_2$  are complex wave numbers in the uncoupled waveguides. We note that the imaginary parts of the wave numbers are related to the Gilbert parameter as  $g_{1,2} = \alpha\omega/v_{g1,2}$ .

Equations (3) determine the waveguide modes of the coupled waveguide system, which are defined as the eigenstates of the matrix  $\hat{M}$ ,

$$\mathbf{e}_{1,2} = (a_1, a_2) = \left( \frac{q_1 - q_2}{2\kappa} \pm \frac{1}{2\kappa} \sqrt{(q_1 - q_2)^2 + 4\kappa^2}, 1 \right), \quad (4a)$$

and the complex wave numbers,

$$Q_{1,2} = K_{1,2} + iG_{1,2} = \frac{q_1 + q_2}{2} \pm \frac{1}{2} \sqrt{(q_1 - q_2)^2 + 4\kappa^2}, \quad (4b)$$

where  $K_{1,2}$  and  $G_{1,2}$  are the real and imaginary parts of the wave numbers in the coupled waveguides. In terms of the averages  $\bar{k} = (k_1 + k_2)/2$ ,  $\bar{g} = (g_1 + g_2)/2$  and differences  $\Delta k = k_1 - k_2$ ,  $\Delta g = g_1 - g_2$ , Eq. (4b) can be rewritten as

$$Q_{1,2} = \bar{k} + i\bar{g} \pm \frac{1}{2} \sqrt{4\kappa^2 + \Delta k^2 - \Delta g^2 + 2i\Delta k\Delta g}. \quad (5)$$

The difference of the wave numbers is

$$\Delta Q = \sqrt{4\kappa^2 + \Delta k^2 - \Delta g^2 + 2i\Delta k\Delta g}. \quad (6)$$

The EP [4,9] occurs when the real and imaginary parts of the wave numbers are equal and the two waveguide modes coincide [5,6,12,17,19]. These conditions hold true at  $\Delta Q = 0$ , which is possible only at  $\Delta k = 0$ . In this case, Eq. (5) is modified to

$$Q_{1,2} = \bar{k} + i\bar{g} \pm \frac{1}{2} \sqrt{\kappa^2 - \Delta g^2}. \quad (7)$$

At  $\kappa^2 > \Delta g^2$ , the wave numbers  $Q_{1,2}$  have different real and equal imaginary parts. In this case, one of the waveguide modes is symmetric, and the other is antisymmetric. When spin waves propagate along the magnonic waveguides, energy oscillations between the waveguides occur. The length of oscillations is determined by the inverse difference of real parts of the wave numbers ( $L_0 = \pi/\text{Re } \Delta Q$ ). In the other case,  $\kappa^2 < \Delta g^2$ , the expression under the square root in (7) assumes a negative value,

so that the wave numbers  $Q_{1,2}$  differ in imaginary parts. Instead of being symmetric or antisymmetric, the eigenmodes are localized in one or other waveguide. In this case, the energy does not oscillate between the waveguides, that is, the length of oscillations  $L$  is infinite. Thus, a pure decay of the spin waves in the waveguides is observed.

In a real system, the condition for EP existence ( $\Delta Q = 0$ ) may be unattainable [49]. This is due to the fact that the variation of imaginary parts of the wave numbers almost inevitably leads to a change in the real parts of wave numbers. As a result,  $\Delta k$  is not zero, and the condition of the EP existence ( $\Delta Q = 0$ ) is not met exactly. However, a change in the system parameters may guide the system in some vicinity of the EP, and a transition from the energy oscillations to decay can be observed. In the current paper, we experimentally demonstrate such a transition in a system of two magnonic waveguides covered by GaAs semiconductor films. An optical IR illumination of one of the waveguides is used to control losses, thereby changing the value of  $\Delta g$ . BLS measurements of the magnetic moment distributions in the waveguides show a qualitative picture of the EP transition. Further, the modal wave numbers, which were directly retrieved from the experimental data, exhibit a convincing picture characteristic of the EP transition.

### III. EXPERIMENTAL METHODS

For the EP observation, lateral magnonic waveguides were fabricated from YIG film with saturation magnetization  $4\pi M_s = 1750$  G and ferromagnetic resonance linewidth  $\Delta H = 0.54$  Oe at a frequency of 9.7 GHz. Each waveguide was 40 mm in length,  $d = 10$   $\mu\text{m}$  thick, and  $w = 200$   $\mu\text{m}$  wide, and the gap between them was  $t = 40$   $\mu\text{m}$  [Fig. 1(a)]. To produce the adjacent magnonic waveguides  $S_1$  and  $S_2$ , the YIG film was structured using a local laser ablation system (LLAS) based on a YAG:Nd fiber laser with a two-dimensional (2D) galvanometric scanning module (Cambridge Technology 6240H) operating in a pulsed regime with a pulse duration of 50 ns and power of 50 mJ. Semiconductor  $n$ -type GaAs film was used to fabricate the layer, which was then used to compose the YIG/GaAs sandwich structure, since it is one of the most utilized types of semiconductor substrates used in CMOS-based electronics as it has high mobility of charge carriers, direct and wide band gap. LLAS was used to fabricate two trapezoid forms of the GaAs surface with a trapezoid base equal to the width  $w$  of each YIG stripe and the same distance between short bases of the trapezoid equal to the distances between  $S_1$  and  $S_2$ . Figure 1(b) shows the microphotography of the GaAs profile, while Fig. 1(c) demonstrates the microphotography of adjacent YIG stripes ( $S_1$  and  $S_2$ ). A 830 nm CW semiconductor laser (hereinafter referred to as an IR laser) was



used to illuminate the area of the contact between the  $S_2$  waveguide and GaAs.

Our experimental structure, which is known as a magnonic directional coupler, was proposed in [50] and has already found practical applications [51] (see Fig. 1). In our recent work, we have shown that the spin-wave dynamics in such a coupler can be easily changed by the power of the excitation signal, leading to spectacular physical phenomena [44]. In particular, it was shown that the coupling between waveguides can be controlled by spin-wave excitation power.

In the experiment, spin-wave excitation was performed in a waveguide  $S_1$  by an Au microstrip antenna  $1\ \mu\text{m}$  thick and  $30\ \mu\text{m}$  wide. A microwave signal with power  $P_{i1} = -15\ \text{dBm}$  from a synthesized CW generator (Anritsu MG3692C) was applied to the input antenna. The structure was magnetized with an external magnetic field of  $H_0 = 900\ \text{Oe}$  induced by a GMW3472-70 electromagnet and directed along the  $y$  axis to excite a Damon-Eshbach magnetostatic spin wave in the input region of  $S_1$ . Light with a wavelength of  $532\ \text{nm}$  and a power of  $1\ \text{mW}$  generated by single-frequency Excelsior (Spectra Physics) EXLSR-532-200-CDRH laser can be focused to a  $25\text{-}\mu\text{m}$ -diameter beam on the surface of the  $S_1$  or  $S_2$  waveguide.

The stationary spatial distribution of dynamic magnetization was studied by the BLS method, which is based on the effect of inelastic light scattering on coherently excited magnons. This corresponds to the linear regime of spin wave excitation and propagation. To obtain maps of the spatial distribution of magnetization, a precision positioning system was used. The IR laser was rigidly connected with the positioning system and was focused into an elliptical shaped spot using a cylindrical lens on the whole area of the  $S_2$  stripe as shown in Fig. 1(a). The experiment was carried out in a quasi-backscattering configuration; the optical signal intensity was proportional to the square of the dynamic out-of-plane component of magnetization in the spatial region, where the laser beam was focused on the magnonic stripe from the side of the Gadolinium Gallium Garnet (GGG) substrate. Maps of spin wave intensity were measured over an area of  $0.5 \times 4\ \text{mm}^2$  within the contact of the YIG stripes with the adjacent GaAs slabs.

#### IV. EXPERIMENTAL RESULTS AND NUMERICAL ANALYSIS

##### A. Manifestation of the exceptional point in the results of BLS measurements

To demonstrate the EP phase transition, a series of 2D maps of spin wave intensity were obtained. Firstly, the measurements were carried out in the absence of the IR laser irradiation. Due to dipole-dipole coupling between the two waveguides the spin wave excited in the first waveguide ( $S_1$ ) oscillated in a periodic manner between

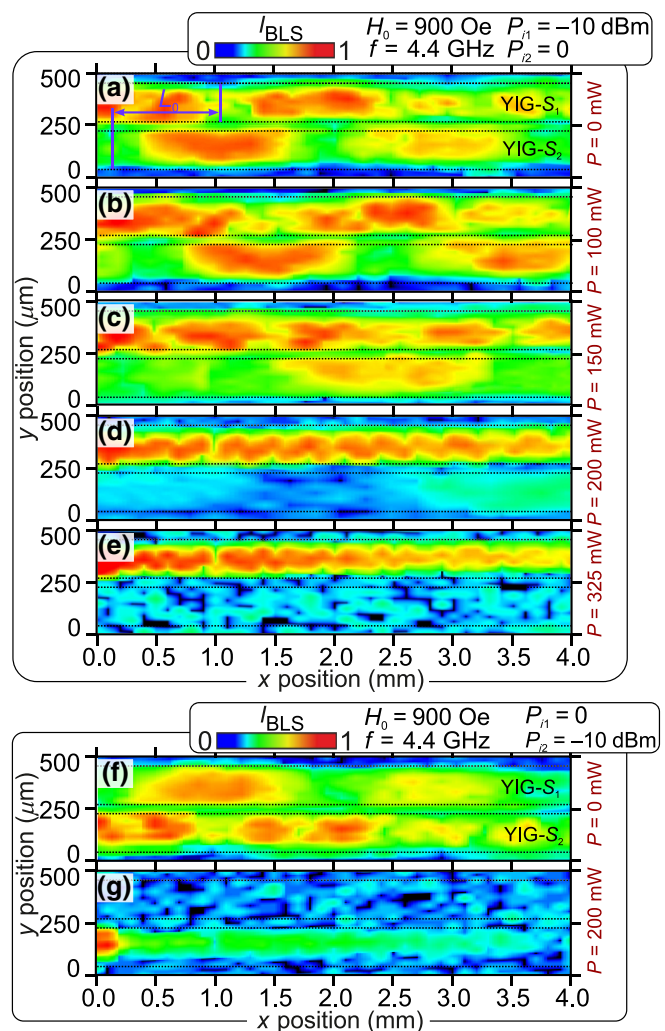


FIG. 2. Series of 2D maps of spin-wave intensity measured with the BLS technique at different levels of CW IR laser power focused with a cylindrical lens on the  $S_2$  waveguide: (a)–(e) the spin wave excited in the first waveguide ( $S_1$ ); (f),(g) the spin wave excited in the second waveguide ( $S_2$ ). The values of the spin wave intensity are given in arbitrary units, and the scale is the same in all the plots. The value of the laser power is shown at the right of each plot.

the two waveguides [Figs. 2(a) and 2(f)]. The oscillation length,  $L_0 = \pi/\Delta K$ , at which the spin wave power transfers from  $S_1$  ( $S_2$ ) to  $S_2$  ( $S_1$ ), is determined by the value of  $\Delta K = \text{Re } \Delta Q$ . To control the spin-wave propagation along the waveguide system, the  $S_2$  waveguide was exposed to the IR laser radiation. The IR laser radiation induces charge carrier transfer from valence band to conduction band in the GaAs semiconductor layer covering the waveguides. This increases the conductance of semiconductor. Therefore, due to variation of the boundary conditions at the surface of the  $S_2$  waveguide, both the change in the spin wave's dispersion and an increase in losses in the  $S_2$  waveguide occur. This causes an increase in the

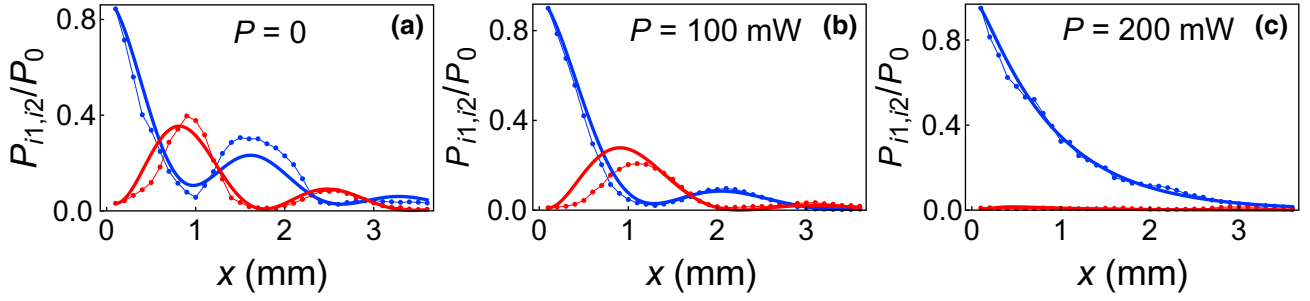


FIG. 3. Spin-wave intensity distributions in the two magnonic waveguides at (a)  $P = 0$ ; (b)  $P = 100$  mW; (c)  $P = 200$  mW. The points show the measured results. Thick lines show the results of simulations with Eq. (3) at the values of parameters that correspond to the minimum square deviation from the experimental data. These parameters are (a)  $\Delta G \approx 6.32 \times 10^{-4}$ ,  $\Delta K \approx 0.377$ , (b)  $\Delta G \approx 1.44 \times 10^{-2}$ ,  $\Delta K \approx 0.292$ , (c)  $\Delta G \approx 0.654$ ,  $\Delta K \approx 0.079$ . The blue and red curves correspond to the  $S_1$  and  $S_2$  waveguides, respectively.

oscillation length  $L_0$  [see Figs. 2 (b) and (c)]. As the IR laser power reached values near  $P = 200$  mW [Figs. 2(d) and 2(g)], the energy transfer between the waveguides disappeared. The increase in losses in the  $S_2$  waveguide has led to a decrease in the propagation length in this waveguide. This change is clearly seen when comparing spin wave intensities obtained when the first [Fig. 2(d)] or second [Fig. 2(g)] waveguide is excited.

The change in the properties of propagating spin waves was due to an increase in  $\Delta g$  induced by the IR laser signal, so that the value of

$$L_0 = \pi / \text{Re} \sqrt{\kappa^2 + \Delta k^2 - \Delta g^2 + 2i\Delta k \Delta g} \quad (8)$$

also increased. Since the change in imaginary parts of the wave numbers was almost inevitably accompanied by a change in the real parts of wave numbers,  $\Delta k$  did not remain zero, so that the condition of the EP ( $\Delta Q = 0$ ) was not met exactly. As a result, we do not observe a disappearance of oscillations predicted exactly at the EP [22] but an increase in the oscillations period near the EP [Fig. 2(c)]

changing by field redistribution between the waveguides [Fig. 2(d)].

### B. Confirmation of the existence of the exceptional point: numerical analysis

To demonstrate the existence of the EP in a convincing manner, we retrieve the wave numbers of the eigenmodes from the experimental data. To this end, we fit the experimental data for the spin wave intensities by solving Eq. (3). At the first step, we simulate Eq. (3) for the magnonic waveguide system at zero IR laser power ( $P = 0$ ). In this regime, the parameters of the two waveguides coincide. Using the least-squares method, we find the dipole-dipole coupling parameter  $\kappa$  and the imaginary part of complex wave numbers  $g_{1,2}$  which are equal to each other at  $P = 0$ . We choose the fitting parameters at which the best approximation is achieved [see Fig. 3(a)]. At the second step, we simulate Eq. (3) at nonzero power of the IR laser, which is used for irradiation of the  $S_2$  waveguide ( $P > 0$ ). We take into account that  $\kappa$  and  $g_1$  do not depend on  $P$ . Using the least-squares method, we find the imaginary part

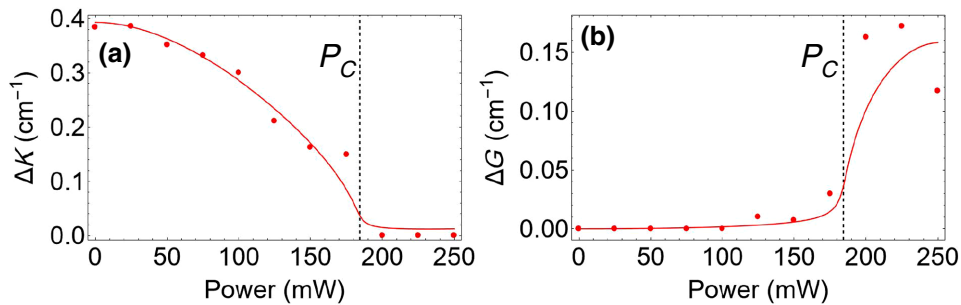


FIG. 4. Dependence of the difference between (a) real and (b) imaginary parts of the wave numbers of the two eigenmodes on the IR laser power  $P$  retrieved from the experimental data (dots) and fitted by Eq. (6) with  $\kappa = 0.197$   $\text{cm}^{-1}$ ,  $\Delta g = \xi_1 P - \xi_2 P^2$ ,  $\xi_1 = 3.37 \times 10^{-3}$   $\text{cm}^{-1} \text{mW}^{-1}$ ,  $\xi_2 = 6.70 \times 10^{-6}$   $\text{cm}^{-1} \text{mW}^{-2}$ ,  $\Delta k = \chi P$ , and  $\chi = 1.86 \times 10^{-5}$   $\text{cm}^{-1} \text{mW}^{-1}$ . Power  $P = P_C$  corresponding to the phase transition is shown by the vertical dotted line.

of the complex wave number in the  $S_2$  waveguide,  $g_2$ , and the difference between the real parts of the complex wave numbers in the  $S_1$  and  $S_2$  waveguides,  $\Delta k$ . Using the parameters found and Eq. (4b), we calculate the values of  $\Delta K$ ,  $G_1$ , and  $G_2$  at each value of the IR laser power (Fig. 4).

The data obtained for  $\Delta K$  and  $\Delta G$  (dots in Fig. 4) are fitted by Eq. (6) (curves in Fig. 4) with an assumption of quadratic dependence of  $\Delta g$  on the IR laser intensity,  $\Delta g = \xi_1 P - \xi_2 P^2$ ,  $\xi_2$  describing the absorbance saturation in GaAs, and with  $\Delta k$  depending linearly on  $P$ , which implies the waveguides' identity at  $P = 0$ . We observe that  $\Delta K$  becomes small at the IR laser power  $P$  below some  $P_C$  [Fig. 4(a)], whereas a significant difference between the decay rates,  $\Delta G$ , appears above  $P_C$  [Fig. 4(b)]. The power corresponding to the phase transition,  $P_C = 184$  mW, was found numerically by a minimization of  $|\Delta Q|$  in Eq. (6).

Besides the change in the wave numbers, the distributions of spin waves in the waveguide eigenmodes are also changed close to the EP phase transition. At the EP, the waveguide eigenmodes coincide. When the system parameters move away from the EP, the waveguide eigenmodes become essentially different from each other. To determine the EP in terms of the eigenmodes, the so-called  $c$ -product is used [4,52]. The  $c$ -product for each of the eigenmodes is determined as  $\langle \mathbf{e}_L | \mathbf{e}_R \rangle$  [4,52], where  $|\mathbf{e}_L\rangle$  and  $|\mathbf{e}_R\rangle$  are the left and right eigenvectors of the matrix  $\hat{M}$  in Eq. (3). That is,  $\hat{M}|\mathbf{e}_R\rangle = \lambda|\mathbf{e}_R\rangle$  and  $\langle \mathbf{e}_L | \hat{M} = \langle \mathbf{e}_L | \lambda$ , where  $\lambda$  is one of the eigenvalues of matrix  $\hat{M}$ . The  $c$ -product  $\langle \mathbf{e}_L | \mathbf{e}_R \rangle$  is calculated by the componentwise multiplication of components of left and right eigenvectors with the same eigenvalues. It is known that at the EP, the  $c$ -product for each of the coincident eigenmodes becomes equal to zero [4,29,52]. This means that these eigenmodes are self-orthogonal at the EP [4,52]. The dependence of the  $c$ -product on the IR laser power can be used as additional proof of the existence of an EP in the system [29].

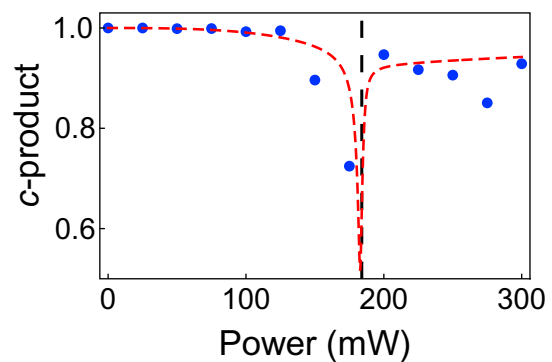


FIG. 5. Dependence of the  $c$ -product for one of the waveguide eigenmodes. The vertical dashed line shows the IR laser power  $P = P_C$ . The dependence of the  $c$ -product for the other waveguide eigenmodes is the same. The dashed red line is a dependence of the  $c$ -product on the IR laser power calculated by using the dependences for  $\Delta K$ ,  $\Delta G$ ,  $\kappa$  obtained by fitting the experimental data.

We retrieve the waveguide modes from the experimental data and calculate the  $c$ -products. Our calculations show that the  $c$ -product for each of the modes has a minimum at the same value of IR laser power equal to  $P_C$  (Fig. 5). Based on this dependence, we conclude that at  $P_C$ , the maximal degree of nonorthogonality of the eigenmodes is achieved. This serves as the second argument for the existence of the EP at the IR laser power of  $P_C$ .

Thus, the dependences of the real and imaginary parts of the wave numbers on the IR laser power indicate the existence of an EP in the system. A similar conclusion follows from the dependences of the  $c$ -product for each of the modes on the IR laser power. All these dependences indicate that the passing near the EP occurs at an IR laser power of  $P_C = 184$  mW. The passing near the EP leads to the transition from energy oscillations between the waveguides to the pure decay of the spin wave intensity. This change is clearly visible in the maps of spin wave intensity measured by BLS techniques.

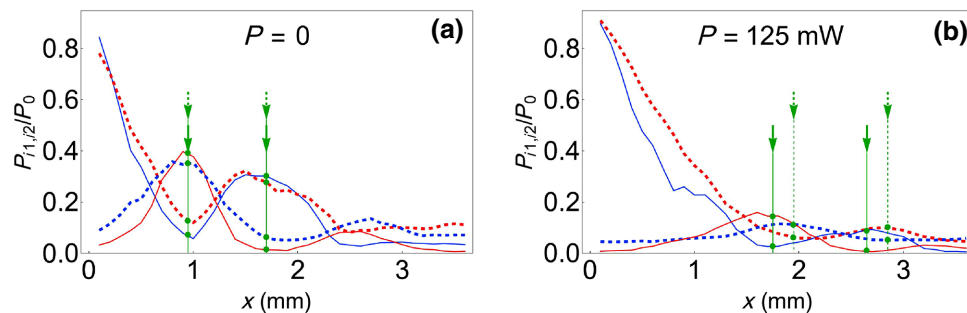


FIG. 6. Spin-wave intensity distributions in the two magnonic waveguides at (a)  $P = 0$ , (b)  $P = 125$  mW measured under the excitation of the  $S_1$  (solid curves) and  $S_2$  (dashed curves) waveguides. In the both cases, the  $S_2$  waveguide was irradiated by the IR laser. The blue and red curves correspond to the  $S_1$  and  $S_2$  waveguides, respectively. The solid and dashed arrows show the positions of the maxima/minima of the spin-wave intensity in the  $S_1$  and  $S_2$  waveguides, respectively.

### C. Nonreciprocal spin-wave behavior below the exceptional point

We have observed a nonreciprocal behavior below the EP, as predicted in [22]. At  $P = 0$ , the waveguides are identical to each other and, therefore, the eigenstates are symmetrical and antisymmetrical. In this case, the intensity distribution of the spin waves is symmetrical with respect to the permutation of the waveguides [cf. Figure 6(a)]. At  $0 < P < P_C$ , the eigenstates are nonorthogonal, so that the intensity distribution of the spin waves becomes non-symmetrical. This change in the eigenstates leads to a nonreciprocal response, which consists in the difference in the positions of the maxima and minima of the spin-wave intensity under the excitation in the  $S_1$  and  $S_2$  waveguides [compare the positions of arrows in Figs. 6(a) and 6(b)].

### V. CONCLUSIONS

We have demonstrated the exceptional-point phase transition in a system of two coupled magnonic waveguides. Using an IR laser irradiation to control the spin-wave parameters in one of the waveguides, we have observed a change in the spin-wave propagation from oscillation between the waveguides to pure decay. From the experimental data, we find the parameters of the propagating spin waves for different powers of the excitation signal. To illustrate the existence of the EP, we track the difference between the wave numbers and demonstrate that in our case at a IR laser power of  $P = P_C \approx 184$  mW this difference is minimal. This proves the passage of the parameters of the magnonic system near the EP. In addition, we calculate the  $c$ -product for each of the waveguide eigenmodes based on the experimental results. It is known that at the EP, the eigenmodes are self-orthogonal [4,52], that is, the  $c$ -product becomes zero. In our magnonic system, the  $c$ -product has a minimum at  $P = P_C$  that serves as the second argument for the existence of the EP. The passing near the EP leads to change in the propagation of the spin waves along the two coupled magnonic waveguides, which is clearly visible in the maps of spin wave intensity measured by BLS techniques. Thus, we argue for the existence of the EP phase transition in coupled magnonic waveguides.

### ACKNOWLEDGMENTS

This work was supported by the Russian Science Foundation through the Grant No. 19-19-00607-P. We are grateful to I. V. Fedosov for a fruitful discussion on the details of optical focusing of IR radiation on a structure.

[1] C. M. Bender and S. Boettcher, Real Spectra in Non-Hermitian Hamiltonians Having PT Symmetry, *Phys. Rev. Lett.* **80**, 5243 (1998).

- [2] C. M. Bender, D. C. Brody, and H. F. Jones, Complex Extension of Quantum Mechanics, *Phys. Rev. Lett.* **89**, 270401 (2002).
- [3] C. M. Bender, Making sense of non-Hermitian Hamiltonians, *Rep. Prog. Phys.* **70**, 947 (2007).
- [4] N. Moiseyev, *Non-Hermitian quantum mechanics* (Cambridge University Press, Cambridge, 2011).
- [5] M. A. Miri and A. Alu, Exceptional points in optics and photonics, *Science* **363**, eaar7709 (2019).
- [6] S. Özdemir, S. Rotter, F. Nori, and L. Yang, Parity-time symmetry and exceptional points in photonics, *Nat. Mater.* **18**, 783 (2019).
- [7] S. W. Hell and J. Wichmann, Breaking the diffraction resolution limit by stimulated emission: stimulated-emission-depletion fluorescence microscopy, *Opt. Lett.* **19**, 780 (1994).
- [8] R. El-Ganainy, K. G. Makris, D. N. Christodoulides, and Z. H. Musslimani, Theory of coupled optical PT-symmetric structures, *Opt. Lett.* **32**, 2632 (2007).
- [9] S. Klaiman, U. Günther, and N. Moiseyev, Visualization of Branch Points in PT-symmetric Waveguides, *Phys. Rev. Lett.* **101**, 080402 (2008).
- [10] K. G. Makris, R. El-Ganainy, D. N. Christodoulides, and Z. H. Musslimani, Beam Dynamics in PT Symmetric Optical Lattices, *Phys. Rev. Lett.* **100**, 103904 (2008).
- [11] Z. H. Musslimani, K. G. Makris, R. El-Ganainy, and D. N. Christodoulides, Optical Solitons in PT Periodic Potentials, *Phys. Rev. Lett.* **100**, 030402 (2008).
- [12] A. Guo, G. J. Salamo, D. Duchesne, R. Morandotti, M. Volatier-Ravat, V. Aimez, G. A. Siviloglou, and D. N. Christodoulides, Observation of PT-Symmetry Breaking in Complex Optical Potentials, *Phys. Rev. Lett.* **103**, 093902 (2009).
- [13] S. Longhi, Bloch Oscillations in Complex Crystals with PT Symmetry, *Phys. Rev. Lett.* **103**, 123601 (2009).
- [14] H. Ramezani, T. Kottos, R. El-Ganainy, and D. N. Christodoulides, Unidirectional nonlinear PT-symmetric optical structures, *Phys. Rev. A* **82**, 043803 (2010).
- [15] C. E. Rüter, K. G. Makris, R. El-Ganainy, D. N. Christodoulides, M. Segev, and D. Kip, Observation of parity-time symmetry in optics, *Nat. Phys.* **6**, 192 (2010).
- [16] A. Regensburger, C. Bersch, M. A. Miri, G. Onishchukov, D. N. Christodoulides, and U. Peschel, Parity-time synthetic photonic lattices, *Nature* **488**, 167 (2012).
- [17] A. A. Zyablovsky, A. P. Vinogradov, A. A. Pukhov, A. V. Dorofeenko, and A. A. Lisyansky, PT-symmetry in optics, *Phys.-Uspekhi* **57**, 1063 (2014).
- [18] L. Feng, R. El-Ganainy, and L. Ge, Non-Hermitian photonics based on parity-time symmetry, *Nat. Photon.* **11**, 752 (2017).
- [19] R. El-Ganainy, K. G. Makris, M. Khajavikhan, Z. H. Musslimani, S. Rotter, and D. N. Christodoulides, Non-Hermitian physics and PT symmetry, *Nat. Phys.* **14**, 11 (2018).
- [20] J. Zhang, B. Peng, Ş. K. Özdemir, K. Pichler, D. O. Krimer, G. Zhao, F. Nori, Y.-X. Liu, S. Rotter, and L. Yang, A phonon laser operating at an exceptional point, *Nat. Photon.* **12**, 479 (2018).
- [21] H. Liu, D. Sun, C. Zhang, M. Groesbeck, R. Mclaughlin, and Z. V. Vardeny, Observation of exceptional points



- in magnonic parity-time symmetry devices, *Sci. Adv.* **5**, eaax9144 (2019).
- [22] X. G. Wang, G. H. Guo, and J. Berakdar, Steering magnonic dynamics and permeability at exceptional points in a parity–time symmetric waveguide, *Nat. Commun.* **11**, 5663 (2020).
- [23] J. Zhao, Y. Liu, L. Wu, C.-K. Duan, Y.-X. Liu, and J. Du, Observation of Anti-PT-Symmetry Phase Transition in the Magnon-Cavity-Magnon Coupled System, *Phys. Rev. Appl.* **13**, 014053 (2020).
- [24] C. Zhao, R. Peng, Z. Yang, S. Chao, C. Li, Z. Wang, and L. Zhou, Nonreciprocal amplification in a cavity magnonics system, *Phys. Rev. A* **105**, 023709 (2022).
- [25] E. J. Bergholtz, J. C. Budich, and F. K. Kunst, Exceptional topology of non-Hermitian systems, *Rev. Mod. Phys.* **93**, 015005 (2021).
- [26] T. T. Sergeev, A. A. Zyablovsky, E. S. Andrianov, A. A. Pukhov, Y. E. Lozovik, and A. P. Vinogradov, A new type of non-Hermitian phase transition in open systems far from thermal equilibrium, *Sci. Rep.* **11**, 24054 (2021).
- [27] M. Liertzer, L. Ge, A. Cerjan, A. D. Stone, H. E. Türeci, and S. Rotter, Pump-Induced Exceptional Points in Lasers, *Phys. Rev. Lett.* **108**, 173901 (2012).
- [28] I. V. Doronin, A. A. Zyablovsky, E. S. Andrianov, A. A. Pukhov, and A. P. Vinogradov, Lasing without inversion due to parametric instability of the laser near the exceptional point, *Phys. Rev. A* **100**, 021801 (2019).
- [29] A. A. Zyablovsky, I. V. Doronin, E. S. Andrianov, A. A. Pukhov, Y. E. Lozovik, A. P. Vinogradov, and A. A. Lisyansky, Exceptional points as lasing prethresholds, *Laser Photonics Rev.* **15**, 2000450 (2021).
- [30] S. Longhi, PT-symmetric laser absorber, *Phys. Rev. A* **82**, 031801 (2010).
- [31] B. Peng, Ş. K. Özdemir, S. Rotter, H. Yilmaz, M. Liertzer, F. Monifi, C. M. Bender, F. Nori, and L. Yang, Loss-induced suppression and revival of lasing, *Science* **346**, 328 (2014).
- [32] L. Feng, Z. J. Wong, R. M. Ma, Y. Wang, and X. Zhang, Single-mode laser by parity-time symmetry breaking, *Science* **346**, 972 (2014).
- [33] H. Hodaei, M. A. Miri, M. Heinrich, D. N. Christodoulides, and M. Khajavikhan, Parity-time–symmetric microring lasers, *Science* **346**, 975 (2014).
- [34] H. Hodaei, A. U. Hassan, S. Wittek, H. Garcia-Gracia, R. El-Ganainy, D. N. Christodoulides, and M. Khajavikhan, Enhanced sensitivity at higher-order exceptional points, *Nature* **548**, 187 (2017).
- [35] J. Wiersig, Enhancing the Sensitivity of Frequency and Energy Splitting Detection by Using Exceptional Points: Application to Microcavity Sensors for Single-Particle Detection, *Phys. Rev. Lett.* **112**, 203901 (2014).
- [36] W. Chen, Ş. K. Özdemir, G. Zhao, J. Wiersig, and L. Yang, Exceptional points enhance sensing in an optical microcavity, *Nature* **548**, 192 (2017).
- [37] M. Zhang, W. Sweeney, C. W. Hsu, L. Yang, A. D. Stone, and L. Jiang, Quantum Noise Theory of Exceptional Point Amplifying Sensors, *Phys. Rev. Lett.* **123**, 180501 (2019).
- [38] Z. Lin, H. Ramezani, T. Eichelkraut, T. Kottos, H. Cao, and D. N. Christodoulides, Unidirectional Invisibility Induced by PT-symmetric Periodic Structures, *Phys. Rev. Lett.* **106**, 213901 (2011).
- [39] L. Feng, Y. L. Xu, W. S. Fegadolli, M. H. Lu, J. E. Oliveira, V. R. Almeida, Y.-F. Chen, and A. Scherer, Experimental demonstration of a unidirectional reflectionless parity-time metamaterial at optical frequencies, *Nat. Mater.* **12**, 108 (2013).
- [40] L. Feng, M. Ayache, J. Huang, Y. L. Xu, M. H. Lu, Y. F. Chen, Y. Fainman, and A. Scherer, Nonreciprocal light propagation in a silicon photonic circuit, *Science* **333**, 729 (2011).
- [41] J. C. Slonczewski, Current-driven excitation of magnetic multilayers, *J. Magn. Magn. Mat.* **159**, L1 (1996).
- [42] M. M. Asmar and W.-K. Tse, Interlayer RKKY coupling in bulk Rashba semiconductors under topological phase transition, *Phys. Rev. B* **100**, 014410 (2019).
- [43] A. A. Zyablovsky, E. S. Andrianov, and A. A. Pukhov, Parametric instability of optical non-Hermitian systems near the exceptional point, *Sci. Rep.* **6**, 29709 (2016).
- [44] A. V. Sadovnikov, S. Odintsov, E. Beginin, A. Grachev, V. A. Gubanov, S. Sheshukova, Y. P. Sharaevskii, and S. A. Nikitov, Nonlinear spin wave effects in the system of lateral magnonic structures, *JETP Lett.* **107**, 25 (2018).
- [45] A. V. Sadovnikov, S. A. Odintsov, E. N. Beginin, S. E. Sheshukova, Y. P. Sharaevskii, and S. A. Nikitov, Toward nonlinear magnonics: Intensity-dependent spin-wave switching in insulating side-coupled magnetic stripes, *Phys. Rev. B* **96**, 144428 (2017).
- [46] A. G. Gurevich and G. A. Melkov, *Magnetization Oscillation and Waves* (CRC Press, Boca Raton, FL, 1966).
- [47] J. W. Boyle, S. A. Nikitov, A. D. Boardman, J. G. Booth, and K. Booth, Nonlinear self-channeling and beam shaping of magnetostatic waves in ferromagnetic films, *Phys. Rev. B* **53**, 12173 (1996).
- [48] A. Yariv, Coupled-mode theory for guided-wave optics, *IEEE J. Quantum Electron.* **9**, 919 (1973).
- [49] A. A. Zyablovsky, A. P. Vinogradov, A. V. Dorofeenko, A. A. Pukhov, and A. A. Lisyansky, Causality and phase transitions in PT-symmetric optical systems, *Phys. Rev. A* **89**, 033808 (2014).
- [50] A. V. Sadovnikov, E. N. Beginin, S. E. Sheshukova, D. V. Romanenko, Y. P. Sharaevskii, and S. A. Nikitov, Directional multimode coupler for planar magnonics: Side-coupled magnetic stripes, *Appl. Phys. Lett.* **107**, 202405 (2015).
- [51] Q. Wang, P. Pirro, R. Verba, A. Slavin, B. Hillebrands, and A. V. Chumak, Reconfigurable nanoscale spin-wave directional coupler, *Sci. Adv.* **4**, e1701517 (2018).
- [52] J. D. Rivero and L. Ge, Pseudochirality: A Manifestation of Noether’s Theorem in Non-Hermitian Systems, *Phys. Rev. Lett.* **125**, 083902 (2020).